Spring Technical Meeting
Eastern States Section of the Combustion Institute
March 4-7, 2018
State College, Pennsylvania

Flight Test Demonstration of LED-based Fire Sensors for Space Propulsion Vehicles

Anthony Carmine Terracciano[1,2,], Kyle Thurmond[1,2], Michael Villar[1,2], Justin Urso[1,2], Erik Ninnemann[1,2], Akshita Parupalli[1,2], Zachary Loparo[1,2], Nick Demidovich[3], Jayanta S. Kapat[1,2], Subith S. Vasu[1,2]*

[1] Mechanical and Aerospace Engineering, University of Central Florida, 4000 Central Florida Blvd., Orlando, FL 32816-2450, USA

[2] Center for Advanced Turbomachinery and Energy Research (CATER), University of Central Florida, 4000 Central Florida Blvd., Orlando, FL 32816-2450, USA

[3]FAA Office of Commercial Space Transportation, 800 Independence Ave SW, Washington DC 20591

[*]Corresponding Author Email:subith@ucf.edu

Abstract: Gases which are indicative of combustion and pyrolysis have absorption features in the mid-infrared range. Therefore, it is possible to implement absorption spectroscopy as a detection method to provide real time monitoring of gases in spacecraft. A sensor developed at the University of Central Florida for this purpose was flown on a proof of concept test flight through partnerships with NASA's Columbia Scientific Balloon Facility (CSBF) and the Louisiana State University (LSU) High Altitude Student Payload (HASP). The test flight enabled autonomous operation of the sensor at an altitude of 105,000ft (32km). The sensor utilizes a 4.2 µm light-emitting diode (LED) source, amplitude modulation to characterize CO_2 concentration, and frequency modulation to characterize ambient temperature.

Keywords: Primary Life Support, Fire Detection, Crew Health Monitoring, Space Systems

1. Introduction

As space travel becomes more prevalent, the pressing concern of ensuring the safety of humans and equipment onboard remains. Hazardous gases within space vehicles pose dangers in the forms of toxic environments, and certain species also indicate the presence of fire. Carbon Dioxide (CO_2), for example, is often a byproduct of combustion and is also known to reduce cognitive performance at high enough concentrations, especially in closed environments [1]. Because of the critical role they possess, hazardous gas sensors are expected to perform reliably and accurately within these harsh environments. Current sensors used within space vehicles mainly employ laser-based absorption measurement systems because they are capable of collecting accurate time-resolved measurements of properties of a variety of gaseous species [2]. However, this method is expensive and much more delicate than preferred for the rough conditions in space. Light emitting diodes (LEDs) are an appealing alternative because they are less expensive, are robust enough to withstand extreme environments, and provide ultra stable output while maintaining a lower power consumption. LEDs also require significantly less complex electrical and thermal driver components. An LED-based sensor that operates on the principles of absorption spectroscopy has been designed and undergone several iterations of development. The latest iteration was tested for its abilities to measure CO_2 while aboard a weather balloon through the High Altitude Student Payload (HASP) group.

The LED sensor detected CO_2 through absorption spectroscopy, which uses the attenuation of light at certain wavelengths related to the oscillations of the gases being identified [3]. *Transmittance,* $\boldsymbol{T}$ *(unitless),* is the ratio of the *observed spectral irradiance,* $\boldsymbol{I_{\lambda,x}}$ *(W·cm^{-2}),* and *reference spectral irradiance ,* $\boldsymbol{I_{\lambda,0,x}}$ *(W·cm^{-2})* (1); these components are represented along with the source's native radiant flux, $\boldsymbol{I_{\lambda,0,x_0}}$ *(W·cm^{-2}).* The total transmittance, $\boldsymbol{T}$, may be expressed in a more explicit form as shown in eq. (2). This form utilizes the *spectral line strength,* $\boldsymbol{S_\lambda}$ *(atm^{-1}·cm^{-2}), line shape function,* $\boldsymbol{\phi_\lambda}$ *(cm),* and *mole fraction of the ith species,* $\boldsymbol{\chi_i}$ *(unitless),* integrated over a *pathlength,* $\boldsymbol{x}$ *(cm)*, and *wavelength range,* $\boldsymbol{\lambda}$ *(nm)*; the total transmittance is the summation for each species exhibiting absorption within the wavelength range. These fundamental parameters may be lumped together for convenience and define a *wavelength-specific absorption coefficient,* $\boldsymbol{\alpha_{\lambda,i}}$ *(cm^{-1}),* as shown in eq. (3). For many molecular species of interest, the HITRAN database provides both $\boldsymbol{\phi_\lambda}$ and $\boldsymbol{S_\lambda}$ [4]. For species that cannot be found in the HITRAN database, it is necessary to measure the temperature-dependent absorption characteristics or to utilize other databases.

$$\boldsymbol{T_\lambda} = \left(\frac{\boldsymbol{I_\lambda}}{\boldsymbol{I_{\lambda,0}}}\right) = \exp(-\alpha_{\lambda,i}\mathrm{L}) \tag{1}$$

$$\boldsymbol{T} = \sum_i \int_{\lambda_0}^{\lambda_1} \int_{x_j}^{x_{j+1}} \boldsymbol{exp}(-\boldsymbol{S_\lambda} \cdot \boldsymbol{\phi_\lambda} \cdot \boldsymbol{\chi_i})\, \boldsymbol{dx}\, \boldsymbol{d\lambda} \tag{2}$$

$$\boldsymbol{\alpha_{\lambda,i}} = \boldsymbol{S_\lambda} \cdot \boldsymbol{\phi_\lambda} \cdot \boldsymbol{\chi_i} \tag{3}$$

Within this text is a brief overview of the sensor's design and the balloon test procedure for the sensor's ability to detect CO_2 by establishing a noise floor and expected signal drift. The results obtained from the HASP flight are intended to be used to further improve the sensor so that it may advance in TRL and be utilized in primary life support.

2. Methods / Experimental

A previous iteration of this sensor had already been tested aboard a balloon flight, with the main goal of the design being to show that multiple gases could be analyzed simultaneously. The output of each LED was modulated at a different frequency and combined into a single beam that reached the detector. The setup for this is shown in Figure 1 below. While the sensor was able to function properly and collect data, the beam splitter design was determined to be ineffective because it further reduced the power output of the LEDs; this was not desirable because one of the main weaknesses of using LEDs instead of laser diodes is the lower power output. The design used, while sturdy, was also larger than preferred because of the required electronics. Therefore, the focus was placed on testing a single LED with a stronger signal while consuming less power overall and refining the electronics components.

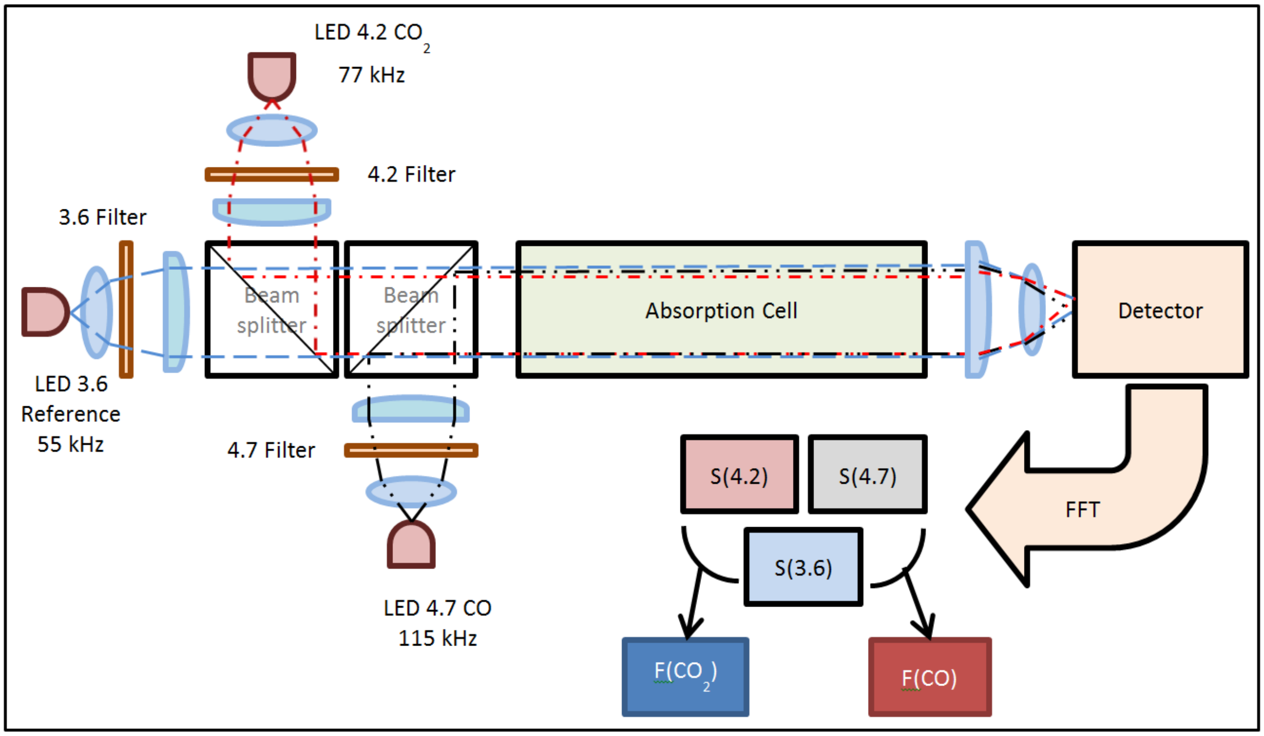

Figure 1: Sensor hardware and processing schematic for previous sensor

Figure 2 below shows the optical path from the LED to the photodiode detector for the current sensor design. The LED, centered around 4.2 μm, served as an emitter. The light first passes through a bi-convex collimating lens before reaching the 4.2 μm filter; the filtered light then passes through a plano-convex lens and a bi-convex lens in order to be collimated to 25mm in diameter before reaching a series of four condenser lenses. The condenser lenses serve to focus the beam onto the photodiode detector.

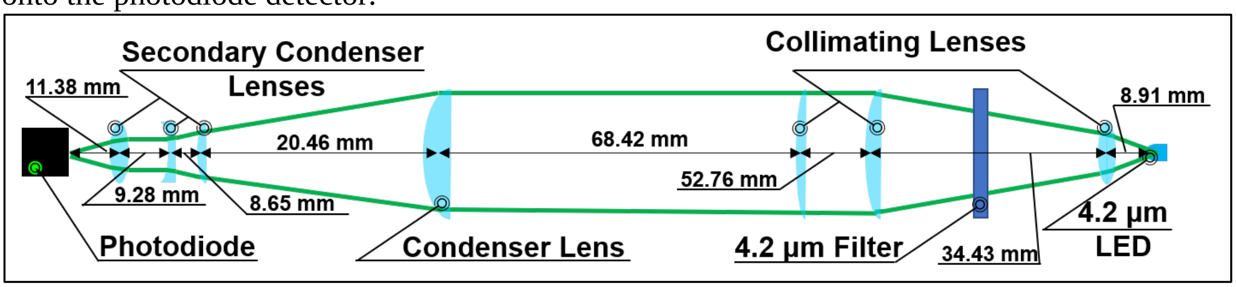

Figure 2: Optical path between LED and detector

A schematic depicting the power usage of the electrical systems is shown in Figure 3 below, while Table 1 shows the power breakdown. The sensor is designed to operate on 30VDC, 0.5A. Therefore, 5 separate DC/DC converters were required to ensure all electronics operated at optimum voltage levels. The National Instruments cRIO-9031 DAQ was used for data acquisition as well as for controlling the sensor and its components.

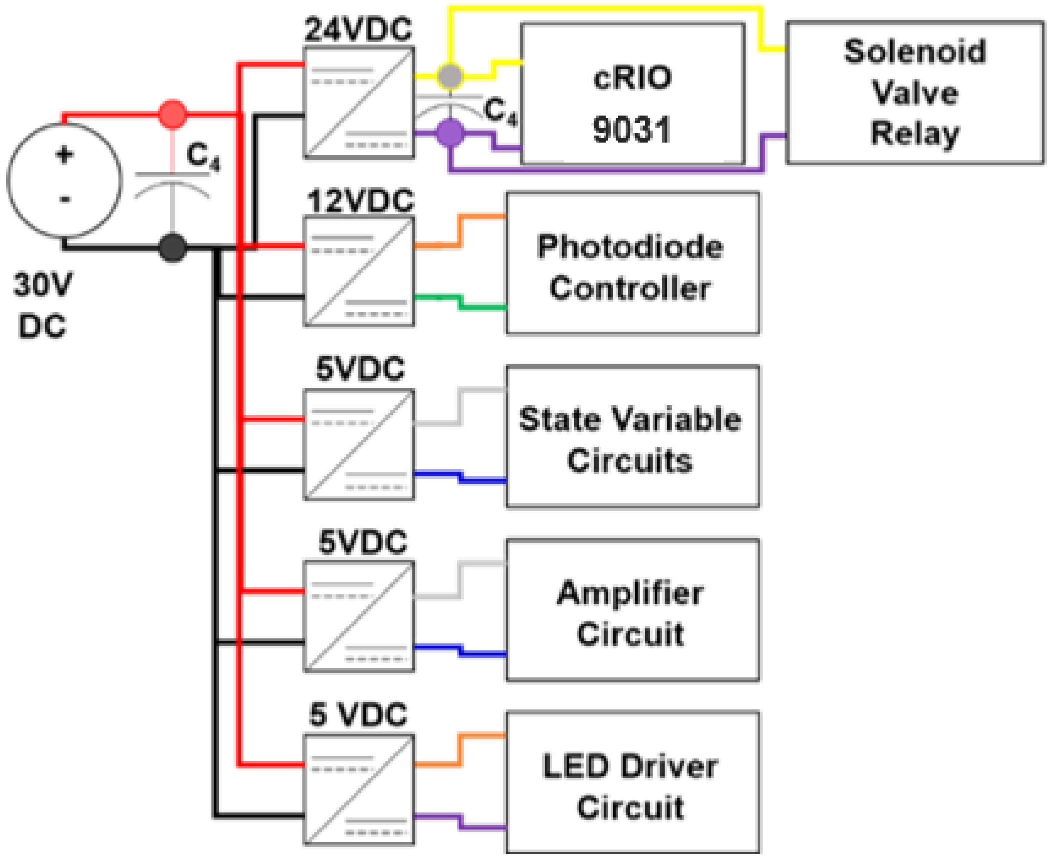

Figure 3: Power breakdown schematic

Table 1: Power Breakdown

Component	Quantity	Voltage	Max Current	Power	Notes
Photodiode Controller	1	12V	1A (2 stage TEC)	12W	Max power, including TEC operation
LED	1	5V	80 mA	0.40W	no TEC operation
cRIO-9031	1	12V	.8A	10W	Max power, continuous operation
Gas Cylinder Solenoid	1	24V	.4A	9.6W	Max power, sporadic operation. Supplemented with capacitors

Figure 4 below shows how the sensor was securely mounted to the HASP weather balloon's platform. Figure 4A shows the outer metal cover, which serves to both secure the sensor to the plate and to assist in radiating heat outward. All electronic and optical components were placed within the acrylic enclosure seen in Figure 4B. The enclosure has been tested to ensure that it is capable of performing in low pressure conditions without allowing air flow. Pressure and temperature within the acrylic enclosure were recorded via the cRIO. Temperatures were recorded using NTC thermistors incorporated into a Wheatstone bridge with a ceramic capacitor across the measurement terminals to mitigate burst noise.

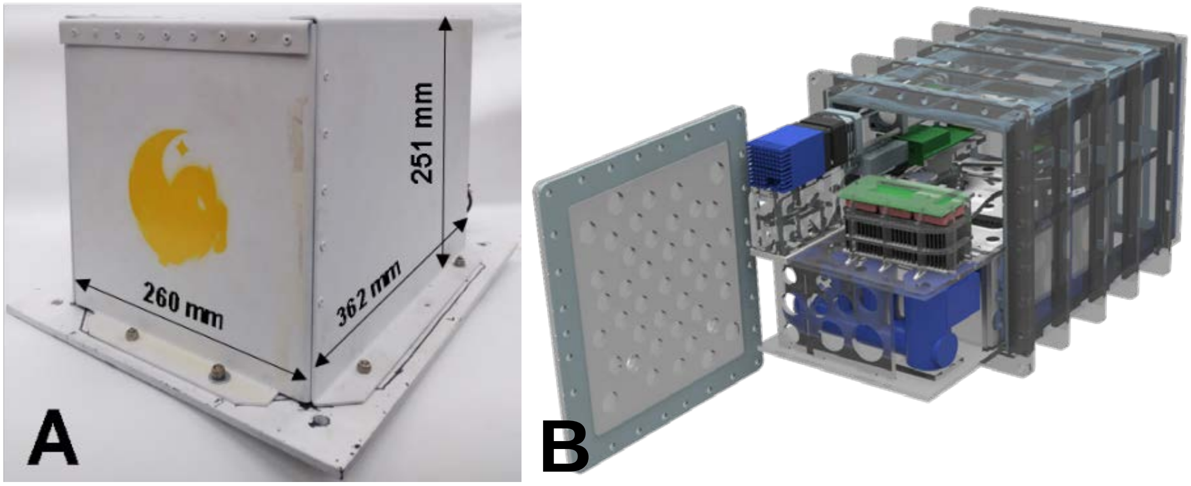

Figure 4: A: Sensor mounted to the HASP platform via an outer metal cover; B: View of the acrylic enclosure and components

3. Conclusions

A CO_2 measurement sensor was tested on a NASA-LSU sponsored high-altitude balloon test flight within an enclosure containing a fixed gas composition as a proof of concept demonstration for use of such a sensor to detect hazardous gases on spacecraft. The testing of the sensor was autonomous where amplitude modulation indicated CO_2 concentration, while frequency modulation was used to reveal temperature within the enclosure. Using ambient air within the sensor as a test gas, a linear curve fit for temperature and CO_2 signal intensity was found with respect to temperature. As this sensor validated its proof-of-concept while reducing power usage, the next iteration will focus on using a rotating grating and multiple LEDs centered around wavelengths of interest in order to test for detection of a larger selection of gases.

5. Acknowledgements

Research at UCF was supported by financial assistance from Federal Aviation Administration Center of Excellence for Commercial Space Transportation (FAA COE-CST) with Ken Davidian as program manager, Florida Space Institute (FSI), NASA Florida Space Grant Consortium (FSGC), the UCF Mechanical and Aerospace Department, and the UCF Office of Research and Commercialization. Z.L. thanks NSF GRFP for partially supporting this effort. The authors would like to thank Dr. Robert Peale (UCF) for assistance with environmental chamber tests.

6. References

1. Satish, U., et al., *Is CO2 an indoor pollutant? Direct effects of low-to-moderate CO2 concentrations on human decision-making performance.* Environmental health perspectives, 2012. **120**(12): p. 1671.
2. Teichert, H., T. Fernholz, and V. Ebert, *Simultaneous in situ measurement of CO, H 2 O, and gas temperatures in a full-sized coal-fired power plant by near-infrared diode lasers.* Applied Optics, 2003. **42**(12): p. 2043-2051.
3. Piatt, U. and J. Stutz, *Differential Optical Absorption Spectroscopy, Principles and Applications*. 2008, Springer, Heidelberg.
4. Rothman, L., et al., *The HITRAN database: 2012 edition.* J Quant Spectrosc Radiat Transfer, 2013.